SPE 13264

SPE
Society of Petroleum Engineers of AIME

ROLE OF ROUGHNESS AND EDGES DURING IMBIBITION IN SQUARE CAPILLARIES

by

Roland Lenormand,
Schlumberger-Doll Research, Ridgefield, Connecticut

Cesar Zarcone,
Institut de Mecanique des Fluides, Toulouse, France

This paper was presented at the 59th Annual Technical Conference and Exhibition of the Society of Petroleum Engineers of AIME, held in Houston, Texas, Sept., 16-19, 1984. The material is subject to correction by the author. Permission to copy is restricted to an abstract of not more than 300 words. Write: P.O. Box 833836, Richardson, Texas 75083.

ABSTRACT

The displacement of one fluid by another in a two-dimensional etched network has been described at the microscopic level: during imbibition, the wetting fluid can flow through the roughness of surfaces, along the edges of the ducts (rectangular cross-section) or in the bulk of the ducts. In this paper, we present results for the time scales of these different mechanisms and the consequences for imbibition in large 2-dimensional networks of capillaries and approximate laws for the flow rates by roughness and corners are calculated in an infinitely long square duct. A theoretical model is built for describing the relationship between the fluid configuration and the Capillary Number (or flow rate):

- ***VERY LOW FLOW RATE:*** *The wetting fluid can reach all the parts of the network by flowing along the surface roughness. It begins to fill the bulk of the smallest ducts and the number of filled ducts increases with time. This is a Cluster growth mechanism.*

- ***LOW FLOW RATE:*** *The wetting fluid can flow along the corners of the ducts but not through the roughness. The mechanism is like Invasion Percolation but the wetting phase flows along the grains of the solid in a special network called: DUAL network.*

- ***HIGH FLOW RATE:*** *The wetting fluid only flows in the bulk of the ducts and the mechanism is a Frontal Drive without fingers nor trapping of the nonwetting phase.*

Printed in U.S.A.

NOMENCLATURE

a	parameter
CA	capillary number in the network
Ca	capillary number in a single channel
Ca_c	capillary number linked to the flow along the corners
Ca_r	capillary number linked to the flow along the roughness
D	numeric coefficient
D_h	hydraulic diameter
d	width of ducts in the network
f	fraction of ducts with a given size d in the network
L	external dimension of the network (width or length)
l	length of the wetting fluid in the small capillaries (roughness)
l^*	dimensionless notation for l
l_o, l_o^*	length of the wetting fluid when the meniscus starts to move
l_∞	asymptotic limit for l
P, P_w	pressure in the wetting fluid
P_c	capillary pressure
P_o	constant pressure at the entrance of the duct
P_p, P_p^*	threshold pressure for the displacement by a piston mechanism
P_s, P_s^*	threshold pressure for the displacement by a snap-off mechanism
P_{I1}, P_{I1}^*	threshold pressure for the displacement by an I1 mechanism
P_{I2}, P_{I2}^*	threshold pressure for the displacement by an I2 mechanism
P_{nw}	pressure in the nonwetting fluid
Q	total volume flow rate in the network
q	volume flow rate in a single channel along the roughness
q_d	volume flow rate in a single channel in the bulk of the duct
q_o	constant volume flow rate in a single channel
n	number of small capillaries in a duct
r	characteristic size of the roughness and diameter of the equivalent capillary
t, t^*	time and dimensionless time
t_o, t_o^*	time when the meniscus starts to flow in the duct
x	depth of the etched ducts in the network, and size of the square single ducts - in Appendix 2, distance from M to the origin
y, y_o	width of the meniscus at point M and at the origin
z	length of the wetting fluid in the bulk of the duct

Greek Symbols:

γ	interfacial tension between the fluids
ΔP	pressure drop between two points
η	ratio between roughness and bulk areas
μ	viscosity of the wetting fluid
ν	parameter linked to the initial shape of the meniscus
θ	contact angle
ξ	distance between two points in the network

13264

ROLE OF ROUGHNESS AND EDGES DURING IMBIBITION IN SQUARE CAPILLARIES

by
Roland Lenormand, Cesar Zarcone

INTRODUCTION

The transport properties (relative permeability, diffusion, thermal or electrical conductivity...) in a porous medium filled with two immiscible fluids are strongly linked to the fluid configuration in the pore space. As is well known, this spatial distribution depends upon the "history" of the sample; for example, the way in which one fluid has been displaced by the other.

In Drainage (wetting fluid displaced by nonwetting fluid), the configuration is studied by using the Invasion Percolation theory[1, 2, 3] and the results are in good agreement with visualizations in 2-dimensional micromodels[4]. However, accurate experiments in real porous media have not yet been performed.

The opposite displacement, called Imbibition, seems to be more complex and visualizations do not agree with the assumptions of theoretical models.

Theoretical studies mainly use the general results of Percolation theory[5, 6] or Invasion Percolation[7], the latter being more suitable for describing the displacement of incompressible fluids. Besides, Invasion percolation has been found to be a very accurate way to get statistical parameters (critical thresholds, universal exponents)[8]. Another approach consists of distributing two phases in the bonds of a network with a percolation process and calculating the relative permeabilities with a Bethe tree model[9, 10, 11]. On the other hand, Koplik and Lasseter[12, 13] do not use percolation concepts but rather describe the displacement and calculate the final saturation for different capillary numbers by a time-step procedure analogous to an electrical network with moving batteries. The common point for all these studies is the very rough description of fluid behavior at the microscopic scale: the main assumptions are that pores or throats are occupied by only one fluid and that menisci move in pores and throats only with respect to their size, as is the case in a circular cross-section capillary.

However, more complex mechanisms have been pointed out. In a theoretical paper[14], a displacement process with two kinds of events is described: a spontaneous rupture of an oil-neck due to instability ("choke-off"), and the spontaneous withdrawal of head menisci out of a pore body ("jump" or "hygron"). Experiments in square cross-section capillaries[15, 16] show that the wetting fluid remains in a triangular area along the corners of the capillaries and that both the fluids can flow simultaneously. Chatzis and Dullien[17] present a critical analysis of the "pore doublet model", used for the interpretation of the trapping of one phase by another during displacement. By using micromodels, they show that trapping during imbibition is strongly linked to the flow of wetting phase in the form of bulk liquid films, which give rise to snap-off of the nonwetting phase at pore constrictions. This kind of mechanism has also been observed in transparent glass etched networks[18, 19, 20] with different pairs of fluids: mercury-air, oil-water, water-air.

The purpose of this paper is to describe all the physical mechanisms observed during imbibition at different flow rates in an etched network, and, taking into account these observations, especially the film flow, to built a general but realistic model. In this study *we don't try to draw a parallel between the etched network and a real porous medium,* but only to understand the real phenomena in a well defined system.

We will show how the spatial distribution of fluids is linked to the following parameters:

- the geometry of the pores and throats;
- fluid properties;
- roughness of the ducts;
- capillary number.

EXPERIMENTAL RESULTS

Micromodels

Glass etched micromodels, used by several laboratories[17, 21], give small pore size and clear observations, but the shape of the cross-section of the ducts is not very well defined. To avoid this problem we have developed a molding technique using a transparent polyester resin and a photographically etched mold[22]. The cross-section of the ducts is rectangular with a constant depth $x = 1$ mm and a width d which varies according to the drawing ($d > 0.1$ mm). A similar technique has recently been used by Mahers

and Dawe[23], to study the mobilization of oil during miscible displacement.

For imbibition experiments we have used a 42,000 duct network with seven classes of width, d, roughly distributed as a log-normal law (the third column in Table 1 gives the fraction, f, of ducts for each size).

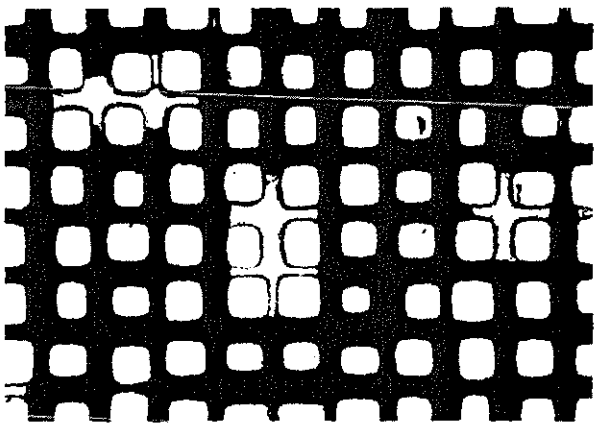

FIG. 1 - Mercury withdrawal in the experimental network (liquid Hg in black).

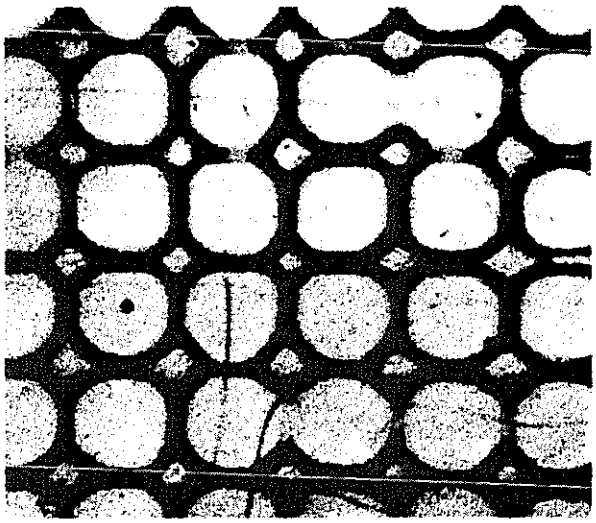

FIG. 2 - Very slow imbibition in a small network with large pores (wetting fluid in black).

Experiments

Experiments are run at different capillary number CA, the ratio between viscous and capillary forces:

$$CA = \frac{Q\mu}{L \times \gamma} \qquad (1)$$

In this equation, μ is the wetting fluid viscosity, γ the surface tension between the fluids, Q the total flow rate in the network and L the width of the network. So, the ratio $Q/L\ x$ is the mean velocity of the injected fluid.

Apart from the mercury withdrawal, all the experiments are run with oil as the wetting fluid (Soltrol) with a dye (oil red O Gurr) and air as the nonwetting fluid. In the pictures, the wetting phase is dark and the nonwetting phase is white.

- Mercury withdrawal.
  The network, previously under vacuum, is filled with liquid mercury. We must increase the pressure in the mercury (nonwetting phase) to make it enter all the pores of the micromodel. Now, by decreasing the pressure (mercury withdrawal), the mercury vapor appears in some ducts to form very compact square or rectangular clusters shown in Fig. 1 (liquid mercury is black and vapor is white). We have shown[24] that this mechanism is similar to an imbibition with two incompressible fluids.

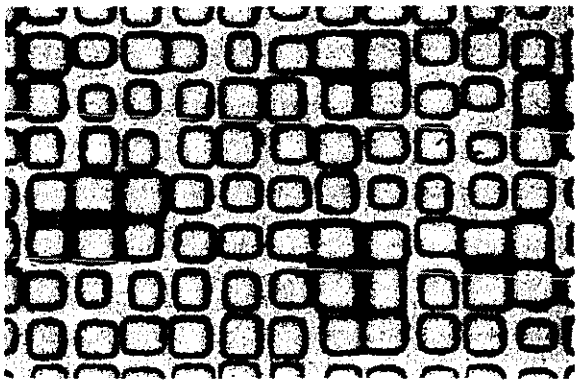

FIG. 3 - Very slow imbibition. Clusters of wetting fluid, in black.

- Very low flow rate ($CA \approx 10^{-9}$).
  Fig. 2 shows an imbibition in a small network with large pores (the distance between two pores is 1.5 mm). Fig. 3, which is a close up of the large micromodel (the distance between pores is 1 mm), shows some ducts filled with the wetting fluid ("clusters") and a small ring of dark fluid around each solid grain.

- $CA \approx 3 \times 10^{-4}$ (Fig. 4a).
  The front is very flat and there is no trapping of the wetting phase.

- $CA \approx 1.4 \times 10^{-5}$ (Fig. 4b).
  There are no clusters but the front is dendritic.

- $CA \approx 6 \times 10^{-7}$ (Fig. 4c).
  A part of the injected fluid seems to be discontinuous (clusters) and the lateral edges of the network facilitate the flow.

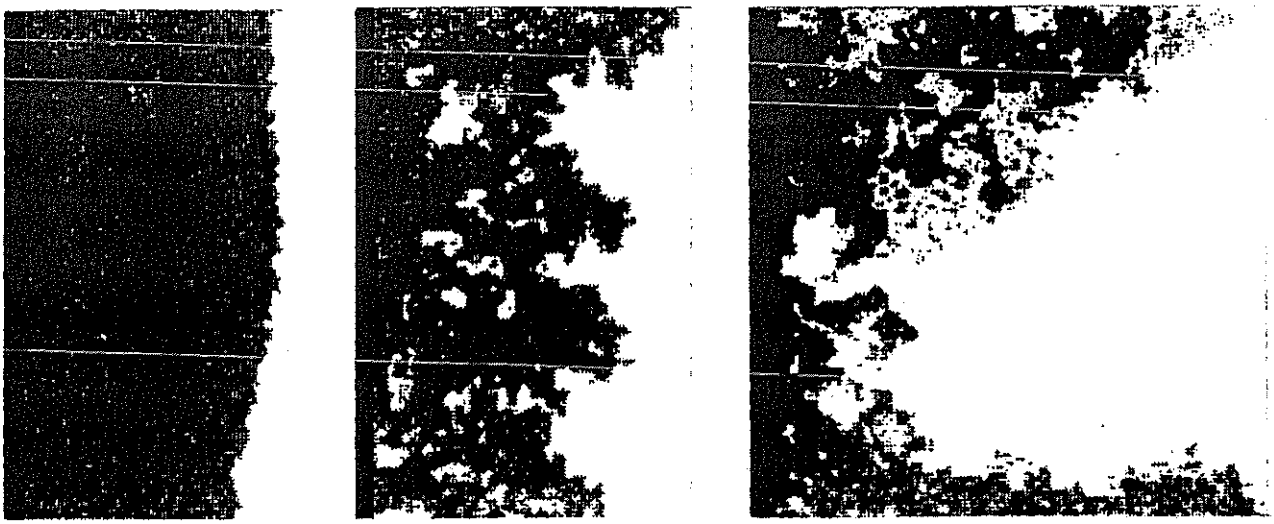

(a) (b) (c)

FIG. 4 - Imbibition in the large network (wetting fluid in black injected on the left). (a) CA = 3×10^{-4}, (b) CA = 1.4×10^{-5}, (c) CA = 6×10^{-7}.

PHYSICAL MECHANISMS

Imbibition is the superposition of three mechanisms:

- the displacement of the interface between the different fluids;
- flow of the nonwetting fluid displaced by the meniscus;
- flow of the wetting fluid from the entrance of the sample to the meniscus.

Novel mechanisms are strongly linked to the noncircular cross-section of the ducts. In fact, experiments show that both fluids can be simultaneously present and flow in the same duct, the wetting fluid remaining in the extreme corners of the cross-section and roughness of the walls (Fig. 5). Let us study these different mechanisms in simple geometries, straight ducts and intersecting ducts.

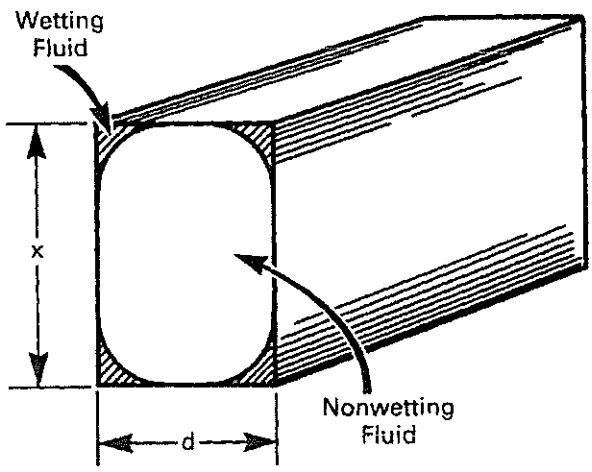

FIG. 5 - Situation of the fluids in a duct.

Meniscus Displacement

This study has been recently published[25,26] and we will only give a summary of the results.

We observe four kinds of displacement of the meniscus during imbibition when the pressure in the wetting fluid increases very slowly and we calculate, for each mechanism, the critical capillary pressure P^* (capillary pressure is the difference between pressures in the nonwetting and the wetting fluid).

- "Piston-type" motion (Fig. 6a).
  The frontal meniscus Σ is inside the duct and the wetting phase displaces the nonwetting phase when the pressure becomes smaller than the capillary pressure in the duct, roughly equal to:

$$\frac{P_p^*}{\gamma} = 2\left(\frac{1}{d}+\frac{1}{x}\right)\cos\theta \qquad (2)$$

- "Snap-off" (Fig. 6b).
  This mechanism has also been called "choke-off" by Mohanty et al[14]. If the frontal meniscus Σ is not inside the duct, the interface moves along the edges as long as its configuration remains steady. The nonwetting fluid has to be in contact with the walls, otherwise an unstable filament is created. The corresponding value for the capillary pressure is:

$$\frac{P_s^*}{\gamma} = \frac{2(\cos\theta - \sin\theta)}{d} \qquad (3)$$

Note that P_p^* is always greater than P_s^*, so the

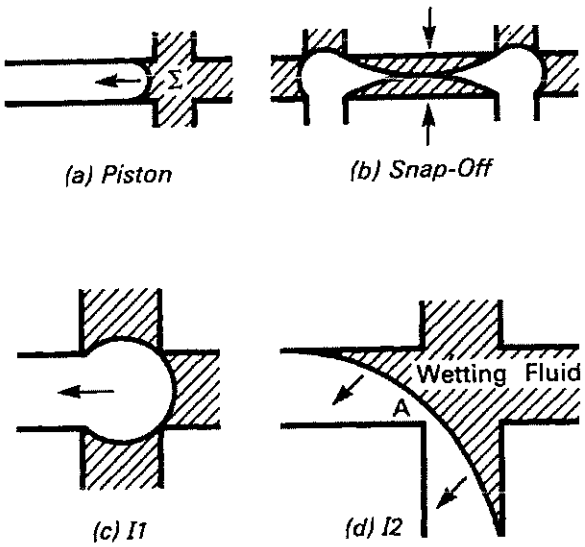

FIG. 6 - Different mechanisms for the meniscus displacement.

"snap-off" only occurs when the "piston" motion is not possible for topological reasons (loop in the nonwetting phase structure, for instance).

- Imbibition "I1" (Fig. 6c).
  The name "I1" means that the nonwetting fluid is only in one duct. When the capillary pressure is decreasing, an instability appears when the meniscus no longer touches the walls. Let us take a special case considering 4 ducts with the same width d :

$$\frac{P_{I1}^{*}}{\gamma} = \frac{\sqrt{2}}{d} + \frac{2\cos\theta}{x} \qquad (4)$$

- Imbibition "I2" (Fig. 6d).
  The nonwetting fluid is in 2 adjacent ducts and the collapse occurs when the meniscus reaches point A at the pressure:

$$\frac{P_{I2}^{*}}{\gamma} = \frac{\cos\theta}{d} - \frac{1}{\sqrt{2}d} + \frac{2\cos\theta}{x} \qquad (5)$$

The other configurations with 3 or 4 ducts filled with the nonwetting phase are very stable and the displacement takes place only by a "snap-off" mechanism in a duct.

All the expressions given previously are only approximations, however they allow us to interpret displacement experiments carried out in etched networks. In Tables 1 and 2 are given the different critical pressures relative to the large network (42,000 ducts) with two different couples of fluids: oil (wetting) and air ($\theta = 0°$) Table 1, and liquid mercury (nonwetting) and vacuum ($\theta = 40°$) Table 2. The depth x of the ducts is constant: x=1 mm.

From these tables we can see that the "piston" displacement always occurs at higher pressure than the other ones, yet it needs a frontal meniscus and consequently it can only take place after another mechanism. All the fluid configurations during Imbibition in a network will be linked to the order in which the different mechanisms take place.

Only with the help of the tables can we predict a different behavior for the oil-air and mercury-vacuum couples when the capillary is slowly decreasing:

- For the oil-air (Table 1), the mechanisms are essentially "snap-off" and "I1", the mechanism "I2" takes place only when the pressure decreases to about 3.9 (P/γ in mm^{-1}) and for this pressure all the others are ended (except for a small fraction of snap-offs in the largest ducts).
- With mercury (Table 2), all mechanisms I1 and I2 take place before snap-off. The amount of wetting fluid in the corners decreases when the contact angle increases and we have shown that 45° is an upper limit[4].

We will see in a following paragraph the consequence for the fluid configurations. So, it is possible to characterize the geometry *and also the effect of contact angle* with three extreme cases:

- "SMALL PORES" when all the "snap-off" pressures are smaller than I1 and I2 pressures:

Table 1

Values of the various displacement pressures P/γ (mm^{-1}) in the experimental network with contact angle $\theta = 0°$.

class	d mm	f	piston	snap-off	"I1"	"I2"
1	.64	.019	5.1	3.1	4.2	2.5
2	.56	.041	5.6	3.6	4.5	2.5
3	.47	.112	6.3	4.3	5.0	2.6
4	.39	.217	7.1	5.1	5.6	2.8
5	.31	.293	8.5	6.5	6.5	3.0
6	.23	.250	10.7	8.7	8.1	3.3
7	.16	.068	14.5	12.5	10.8	3.9

Table 2

Values of the various displacement pressures P/γ (mm^{-1}) in the experimental network with contact angle $\theta = 40°$.

class	d mm	f	piston	snap-off	"I1"	"I2"
1	.64	.019	3.9	.4	3.7	1.6
2	.56	.041	4.3	.4	4.0	1.7
3	.47	.112	4.8	.5	4.5	1.7
4	.39	.217	5.4	.6	5.1	1.7
5	.31	.293	6.5	.8	6.0	1.7
6	.23	.250	8.2	1.1	7.6	1.8
7	.16	.068	11.1	1.5	10.3	1.9

$$(P_{I1}, P_{I2}) > P_s \quad (6)$$

The network with mercury corresponds to this case (Table 2).

- "MEDIUM SIZE PORES" when I2 pressures are below snap-off and I1 pressures:

$$(P_{I1}, P_s) > P_{I2} \quad (7)$$

This is roughly the case for the network with oil and air (Table 1).

- "LARGE PORES" when:

$$P_s > (P_{I1}, P_{I2}) \quad (8)$$

This case corresponds to a large pore at each intersection, the small network shown in Fig. 2, with oil and air,

This description is more accurate than the qualitative concept of "aspect ratio" given by Chatziz et al[18] because it takes into account the real mechanisms linked to the network geometry, and also fluid properties.

Flow of the Nonwetting Phase

The nonwetting fluid can flow only in the bulk of the duct and doesn't see the details of the walls. So the flow occurs only if a continuous path of ducts and intersections filled with this phase exists between the displaced meniscus and the network exit. If there is no continuity, the nonwetting fluid is trapped and the meniscus cannot move.

Flow of the Wetting Phase

During experiments we can see the flow of wetting phase along the corners and roughness and we will try to calculate the order of magnitude of the flow rates linked to these mechanisms. So, we study the imbibition in a single straight channel with a square cross-section (x,x) and infinite length. The pressure remains constant at the entrance and its value corresponds to the capillary pressure in the duct (Eq. 2). The pressure drop in the nonwetting phase is assumed to be negligible, so we will take the nonwetting phase pressure as the reference pressure. Consequently the pressure P in the wetting fluid is negative. At the entrance of the channel:

$$P_o = -\frac{4\gamma}{x} \quad (9)$$

The meniscus doesn't move in the bulk of the duct but the wetting fluid flows along the roughness and corners with respective capillary numbers Ca_r and Ca_c, with the following definition of the capillary number in a duct (the reference length is x):

$$Ca = \frac{q\,\mu}{x^2\,\gamma} \quad (10)$$

The flow rate calculations are detailed in Appendices 1 and 2.

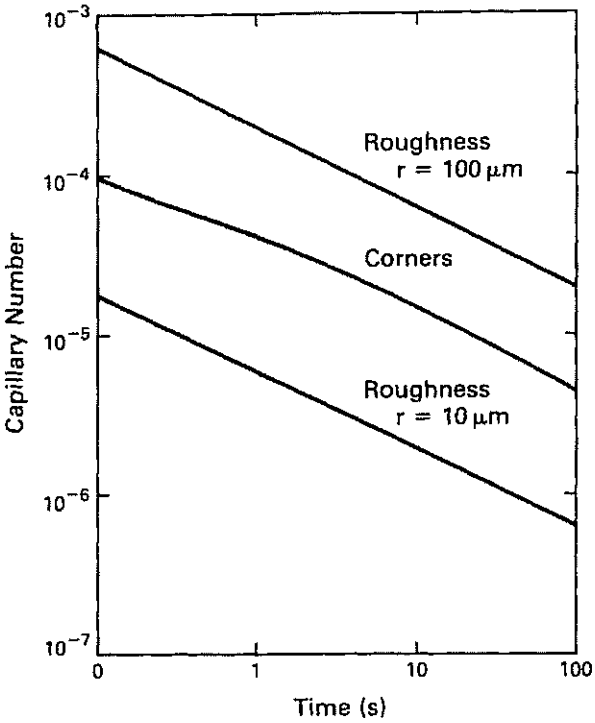

FIG. 7 - Theoretical values for the flow rate by roughness and corners.

- FLOW BY ROUGHNESS. r is the length scale of the roughness:

$$Ca_r = \frac{\pi}{8}\left(\frac{\mu}{\gamma}\right)^{\frac{1}{2}} x^{\frac{1}{2}} \left(\frac{r}{x}\right)^{\frac{3}{2}} t^{-\frac{1}{2}} \quad (11)$$

- FLOW BY CORNERS. The flow rate is deduced from Eq. 52 with 4 corners and initial condition $y_o = x/4$:

$$Ca_c = 2.8\ 10^{-3} \left(\frac{\mu}{\gamma}\right)^{\frac{1}{2}} x^{\frac{1}{2}} t^{-\frac{1}{2}} \quad (12)$$

The ratio between these two capillary numbers (or two flow rates) is only function of duct geometry:

$$\frac{Ca_r}{Ca_c} = 140 \left(\frac{r}{x}\right)^{\frac{3}{2}} \quad (13)$$

For the etched networks the ratio r/x seems of the order of 0.01 ($r \simeq 10\ \mu$m). So the two mechanisms are of the same order of magnitude (ratio = 0.1).

In Fig. 7 are plotted the capillary number versus time on log-log scale for two values of the roughness size ($r = 10\ \mu$m and 100 μm) and the corners (with the exact solution Eq. 51). The parameters correspond to the fluid used during experiments: $\mu = 5$ cP, $\gamma = 20$ dyne/cm, $x = 1$ mm.

We can see that these capillary numbers correspond

to classical displacement in porous media ($10^{-3} - 10^{-6}$).

Experiments in straight ducts with different sizes are in progress and the preliminary results agree with this theoretical approach.

MODELING IN A 2-DIMENSIONAL NETWORK

So far we have examined the displacement of one meniscus at the microscopic scale and the flow of each fluid. From these results we will try to describe the behavior of the wetting fluid injected at constant flow rate in a large network of capillaries.

In the networks many elementary events are possible for a given local capillary pressure but the observations show that they take place one after another and with a well-defined priority: the fastest event occurs first. The time scale is roughly independent of the size of the ducts:

- "Piston" is very fast. The driving force (difference between the local capillary pressure and equilibrium pressure) is very high.
- "Imbibition I1 or I2" is fast. The driving force is low but the viscous forces are small.
- "Snap-off" is very slow because of the high pressure drop in the small path along the corners.

Now, let us consider the different kinds of wetting phase flow (roughness, corners, ducts) and see what configuration can be expected at the network scale. For each kind of flow we will also calculate the characteristic capillary number CA in the network (Eq. 1).

Imbibition With Flow by Roughness

We assume that the flow along roughness in the network is described by the same equations as in a single straight channel and that the total flow Q is equally divided between the ducts. Consequently the capillary numbers (Ca) measured in one duct and in the whole network (CA) are the same.

The flow by roughness is important if the initial length l_o before flow in the bulk of the duct is of the order of the network length L (L=150 mm). Eq. 31 leads to:

$$CA < \frac{\pi}{16}\frac{r^2}{Lx} \approx 10^{-7} \qquad (14)$$

On the other hand, this mechanism becomes negligible if we are in the asymptotic limit (flow in the bulk of the ducts) with a length l_∞ equal to x. Using Eq. 39:

$$CA = \frac{1}{8}\frac{r}{x} \approx 10^{-3} \qquad (15)$$

However, we only see the effect of this kind of flow if snap-off can occur without apparent continuity with the bulk of the wetting fluid. A rough calculation of the pressure drop along the roughness leads to the condition: $CA < 10^{-5}$.

Now, we consider the case where this mechanism is important. The wetting phase can flow everywhere in the network. Progressively the corners are filled and the capillary pressure decreases. If there are no edges along the lateral sides of the network, the only mechanism which can take place is snap-off in the smallest ducts. Let us assume that the pressure drop across the network is small compared to the capillary pressure (with a steady state flow in the roughness, we find $Ca << 10^{-9}$). The result depends upon the relative value of critical pressures for the different kinds of meniscus displacements.

We can compare the results on the small simulation shown in Fig. 8, with the same distribution of duct sizes and same capillary pressure corresponding to 28% of bonds filled by snap-off.

- "LARGE PORES":
  $P_s > (P_{I1}, P_{I2})$ (Fig. 8a).
  All the snap-offs can occur before the I1 and I2

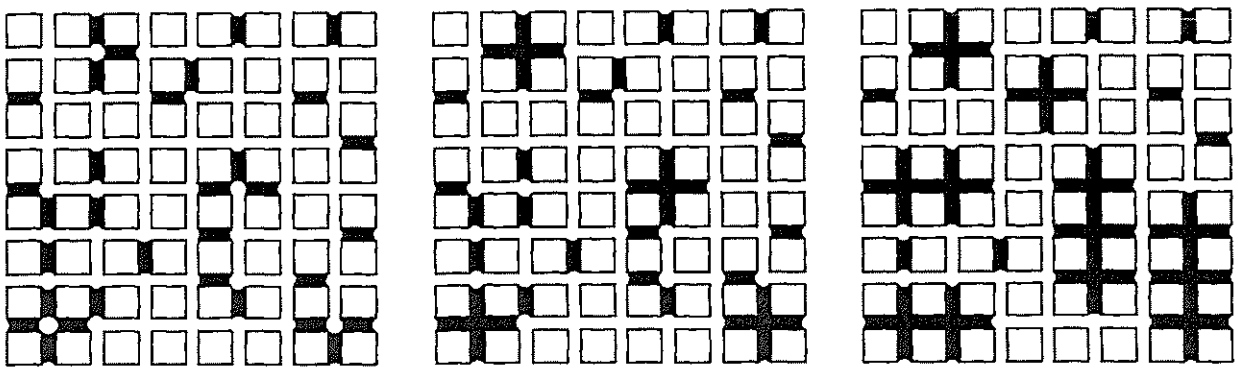

(a) Large Pores (b) Medium Size Pores (c) Small Pores

FIG. 8 - Imbibition with flow along the roughness. Simulations for different pore geometries.

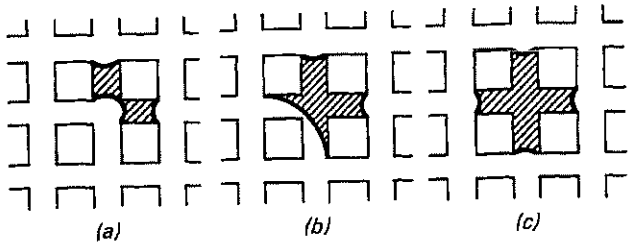

FIG. 9 - Imbibition with flow along the roughness. Formation of compact clusters.

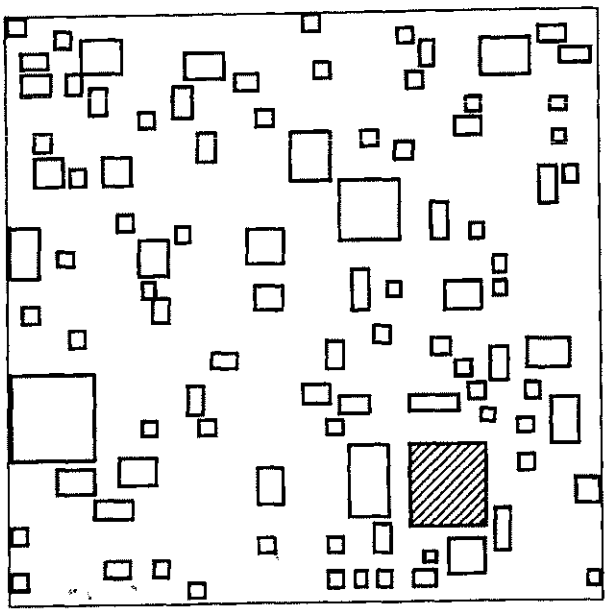

FIG. 10 - Imbibition with flow along the roughness. Simulation of the cluster growth mechanism.

displacements and the number of filled ducts increases with time at random location. Therefore this mechanism is a *CLASSICAL BOND PERCOLATION:* we are cutting bonds in the network until the nonwetting phase becomes discontinuous. The threshold occurs for a given fraction of cut bonds, this fraction being a function of the connectivity (see, e.g.,[27]).

- "SMALL PORES":
  $(P_{I1}, P_{I2}) > P_s$ (Fig. 8c).
  In the absence of lateral edges in the network, the only way for Imbibition to take place is snap-off, but the capillary pressure is very low and when two adjacent ducts are filled (Fig. 9a) the I2 displacement takes place instantaneously (Fig. 9b) and fills the pore and the two other ducts (Fig. 9c). Fig. 10 shows the result of a simulation on a 50 x 50 lattice, the fraction of ducts where snap-off occurs is 0.13 and increasing this fraction leads to an instable behavior, the hatched cluster will grow and invade the whole lattice[24]. In a recent paper[28], we have shown by using computer simulations and statistical theory that this critical fraction is not a percolation threshold but tends to zero as the network size increases. This is a *NUCLEATION CLUSTER GROWTH.*

- "MEDIUM SIZE PORES":
  $(P_{I1}, P_s) > P_{I2}$ (Fig. 8b).
  In this case, imbibition I2 is not possible, but only snap-off and I1. So, when 3 adjacent ducts are filled, the pore and the fourth duct are automatically filled. This case has not been studied but it seems to be also a percolation process with the same threshold as the first one.

Imbibition With Flow Along the Corners

Let us assume, in this theoretical approach, that there is no flow along the roughness (network with smooth ducts) and that the pressure is uniform in the wetting fluid (we will discuss this point later). Simulations with different pore sizes are shown in Fig. 11: (wetting fluid in black).

- "LARGE PORES" (Fig. 11a). As in drainage, the interface moves by a succession of jumps.

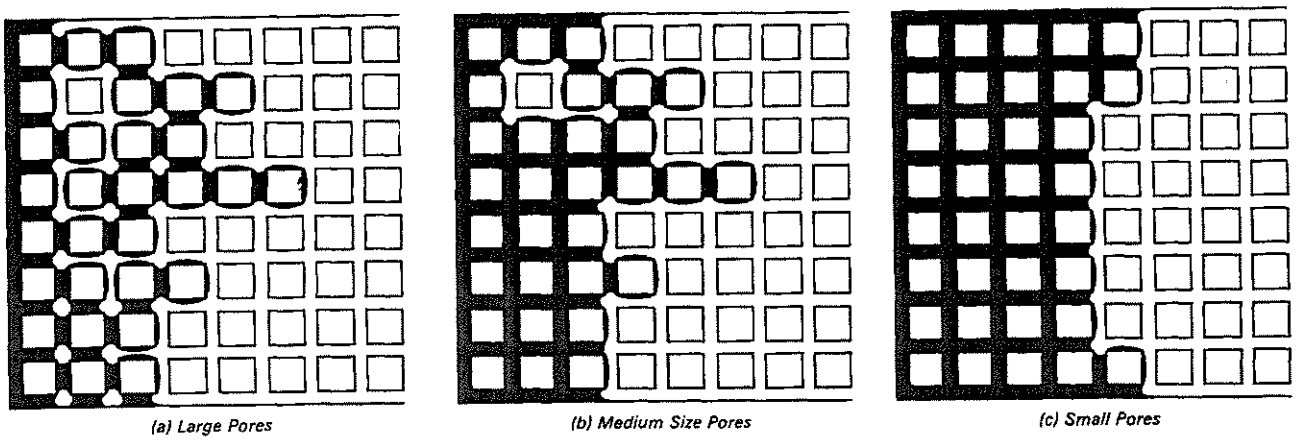

FIG. 11 - Imbibition with flow along the corners. Simulations for different pore geometries.

All the menisci in pores and along corners are at the same pressure which progressively decreases as the wetting fluid is injected (the volume of fluid increases in the corners, therefore the radius of curvature increases). The jump occurs when the pressure reaches the snap-off threshold in the smallest duct on the front. A large amount of fluid is taken by this snap-off and consequently the capillary pressure increases until the next jump takes place.

This mechanism is similar to an "Invasion Percolation" process[7], but the topology is not the same as in Drainage. Fig. 12a shows a close-up of the central part of the network Fig. 11a and Fig. 12b the lattice of bonds and sites equivalent to the ducts and pores, we will call it "primary network". In drainage, invasion percolation is described in this primary network but in imbibition, the continuity between N (where a jump can occur for example) and M is found in the "DUAL" network shown Fig. 12c. The sites of the dual network are the centers (A,B,C...) of the solid grains and the jump by snap-off in N is equivalent to a "bond" connection between sites C and D.

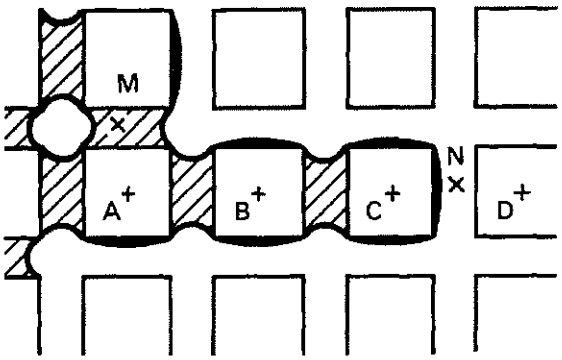

(a) Etched Network

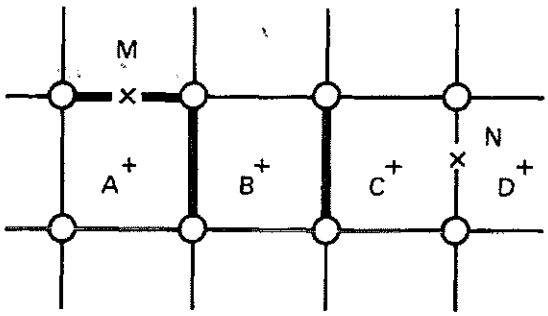

(b) Primary Network

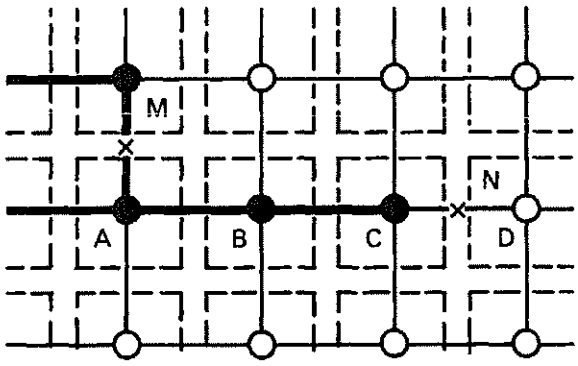

(c) Dual Network

FIG. 12 - Imbibition with flow along the corners. Continuity of the wetting phase in the DUAL network.

This kind of Imbibition can be described as an *INVASION BOND PERCOLATION* in the *DUAL NETWORK*. However, the continuity of the nonwetting phase has to be found in the primary network (this phase flows in the bulk of the ducts).

- "MEDIUM SIZE PORES" (Fig. 11b). The basic mechanism is the same as previously but an I1 displacement occurs when three adjacent ducts are filled. In the dual network this is equivalent to connecting the fourth bond when the three others of a square are connected, and it seems to be a detail at small scale, not relevant for the percolation process.
- "SMALL PORES" (Fig. 11c). Displacement I2 occurs before snap-off. So imbibition is a succession of I2 jumps which fill the network line after line. The result is a *FRONTAL DRIVE* with a very flat front.

Now, we can calculate the time scale for a "quasi-static" percolation. We assume that the pressure drop in a very thin percolation finger is small, compared to the capillary pressure. At threshold, capillary pressure is about $6\gamma/x$ (pressure for class 5 to get a fraction of active bonds larger than 0.5, the percolation threshold in a 2-dimensional square network). From this pressure we calculate the radius of curvature and the hydraulic diameter of an equivalent steady Poiseuille flow. So:

$$CA << 4\ 10^{-6}\ \frac{x^2}{L^2} \approx 10^{-10} \qquad (16)$$

On the other hand, flow along corners become negligible at high capillary numbers. The limit is when only one snap-off occurs when the wetting fluid fills a total line of the network in the frontal drive process (see below). We calculate the characteristic time for snap-off as the time to fill one duct (volume x^3) with the flow rate given by Eq. 52 (with $y_o = x$). During this time the wetting fluid fills a whole line (volume $x^2\ L$). The calculation leads to a capillary number (in the network) equal to 0.03. For smaller flow rate, some snap-off occurs and makes a local perturbation on the flat front of the frontal drive. When

Table 3
Different imbibition mechanisms.

	LARGE PORES	MEDIUM SIZE PORES	SMALL PORES
ROUGHNESS	bond percolation	bond percolation + correlations	nucleation cluster growth
CORNERS	Invasion percolation dual network	Invasion percolation + correlations	frontal drive
BULK OF THE DUCTS	frontal drive	frontal drive	frontal drive

the capillary number decreases, the number of these events increases until a pure percolation process is achieved (for large pores).

Imbibition Only in the Bulk of the Ducts

The only mechanisms are I1 and I2 and whatever the pore size is, the displacement is a *FRONTAL DRIVE,* as described previously.

Let us calculate the pressure drop along a distance ξ in the network with the assumptions of flow in parallel channels and hydraulic diameter:

$$\Delta P \simeq 4 \frac{\gamma}{x} \frac{\xi}{x} 10^2 \, CA \qquad (17)$$

When $CA = 10^{-4}$, the pressure drop along the network is of the order of the capillary pressure $(4\gamma/x)$.

The different results are presented in Table 3.

DISCUSSION

Now, let us compare theory and observations. Experimental results suggest four domains with respect to the capillary number:

- HIGH CAPILLARY NUMBER:
  $CA > 10^{-4}$.
  The wetting fluid flows only in the bulk of the duct. The shape of the frontal drive (Fig. 4a) and also the numerical value of the transition is in good agreement with calculation.

- MEDIUM CAPILLARY NUMBER:
  $10^{-6} < CA < 10^{-4}$.
  Flow by roughness is not important and the flow rate is too high for the flow by corners to lead to a pure percolation process (10^{-10}). Consequently the front is the result of the "cross-over" between the frontal drive and the percolation process. By decreasing the capillary number, the average length of the fingers increases from the pore scale (Fig. 4a) to the length of the network (percolation).

  An accurate observation of menisci along the front in Fig. 4b shows that the radius of curvature is constant. This result agrees with a calculation of the pressure drop in the wetting phase. By using Eq. 17, this pressure drop is found to be smaller than 1% of the capillary pressure.

  This result is very important because it allows us to build a statistical model, as in a quasi-static displacement. So, the cross-over can be studied by increasing the fraction of correlated bonds and sites in an invasion percolation model. This interface behavior will be studied in further publications.

- LOW CAPILLARY NUMBER:
  $10^{-9} < CA < 10^{-6}$.
  Flow along roughness is important but the pressure is nonuniform inside the micromodel (Fig. 4c). Hence, the size of the clusters is linked to the distance from the entrance: very small clusters downstream, and large clusters which join together to form a continuous domain near the entrance.

  We can also note the important effect of the lateral edges of the network. At very low flow rate, the configuration of fluids depends also upon the boundaries and further investigations have to be made.

- VERY LOW CAPILLARY NUMBER:
  $CA < 10^{-9}$.
  In this case, flow by roughness is the most important mechanism for wetting fluid transportation and the theory is in good agreement with the experiments. For mercury withdrawal (Fig. 1), clusters are very compact (square or rectangular) as described by the model for the "small pores" case (Table 2). For oil imbibition (Fig. 3), clusters are not so compact because of some I2 mechanisms which cannot occur and this result agree with the "medium size pore" modelization.

CONCLUSION

This study points out the important role of the flow by roughness and corners of the ducts during imbibition in an etched network:

- The basic or "reference" mechanism is a flat frontal drive without trapping of the nonwetting

phase (value $CA > 10^{-4}$) close to the experimental result published by Morrow and Songkran[29]. However, the shape of the interface is only due to a specific mechanism (called I2 in our study) and not to a viscous pressure drop.

- When the capillary number decreases, the flow by roughness and corners "has enough time" to take place and acts like a "suction" on the interface and consequently the capillary pressure increases along the interface between the fluids, the pressure inside the bulk wetting phase remaining constant.
- The value of the capillary pressure leads to a selection for the mechanisms of meniscus displacement and the shape of the front is a consequence of the kind and the fraction of allowed mechanisms.

ACKNOWLEDGMENT

We wish to thank P. G. de Gennes, E. Guyon, Y. Pomeau and D. Wilkinson for several useful discussions and suggestions and B. Schmidt who assisted with the experimental work. This research was supported in part by Institut Francais du Petrole and Centre National de la Recherche Scientifique.

REFERENCES

[1] Lenormand, R. and Bories, S.: "Description d'un mecanisme de connexion de liaison destine a l'etude du drainage avec piegeage en milieu poreux," *C. R. Acad. Sci.*, Paris (December 8, 1980), **291 b,** 279-281.

[2] Larson, R. G and Morrow, N. R.: "Effects of Sample Size on Capillary Pressures in Porous Media," *Powder Tech.*, (1981), **30,** 123-138.

[3] Chandler, R., Koplik, J., Lerman, K., Willemsen, J. F.: "Capillary Displacement and Percolation in Porous Media," *J. Fluid Mech.*, (June, 1982), **119,** 249-267.

[4] Lenormand, R.: "Deplacements polyphasiques en milieu poreux sous l'influence de forces capillaires. Etude experimentale et modelisation de type percolation," (1981) Doctorat Thesis, Institut National Polytechnique, Toulouse France.

[5] De Gennes, P. G. and Guyon, E.: "Lois generales pour l'injection d'un fluide dans un milieu poreux aleatoire," (1978), *J. Mecanique* **17,** 403-442.

[6] De Gennes, P. G.: "Theory of Slow Biphasic Flows in Porous Media," (1983), *Phys. Chem. Hydro.*, **4,** 175-185.

[7] Wilkinson, D. and Willemsen, J. F.: "Invasion Percolation: A New Form of Percolation Theory," (1983), *J. Phys.* A, **16,** 3365-3376.

[8] Wilkinson, D. and Barsony, M.: "Monte Carlo Study of Invasion Percolation Clusters in Two and Three Dimensions," (1984), *J. Phys.* A, **17,** L129-L135.

[9] Heiba, A. A., Sahimi, M., Scriven, L. E. and Davis, H. T.: "Percolation Theory of Two-Phase Relative Permeability," Paper SPE-11015, presented at the 57th Annual Technical Conference of the SPE, New Orleans, September 26-29, 1982.

[10] Heiba, A. A., Davis, H. T. and Scriven, L. E.: "Effect of Wettability on Two-Phase Relative Permeabilities and Capillary Pressures," Paper SPE-12172, presented at the 58th Annual Technical Conference of the SPE, San Francisco, October 5-8, 1983.

[11] Heiba, A. A., Davis, H. T. and Scriven, L. E.: "Statistical Network Theory of Three-Phase Relative Permeabilities," Paper SPE/DOE-12690, presented at the 4th Symposium on Enhanced Oil Recovery, Tulsa, April 15-18, 1984.

[12] Koplik, J. and Lasseter T. J.: "Two-Phase Flow in Random Network Models of Porous Media," Paper SPE-11014, presented at the 57th Annual Technical Conference of the SPE, New Orleans, September, 26-29, 1982.

[13] Koplik, J. and Lasseter, T. J.: "One- and Two-Phase Flow in Network Models of Porous Media," (1984), *Chem. Eng. Commun.*, **26,** 285-295.

[14] Mohanty, K. K., Davis, T. and Scriven, L. E.: "Physics of Oil Entrapment in Water-Wet Rock," Paper SPE-9406, presented at the 55th Annual Technical Conference of the SPE, Dallas, September 21-24, 1980.

[15] Legait, B.: "Laminar Flow of Two-Phase Through a Capillary Tube with Variable Square Cross-Section," (1983), *J. Colloid Inter. Sci.*, **96,** 28-38.

[16] Arriola, A., Wilhite, G. P. and Green, D. W.: "Trapping of Oil Drops in a Noncircular Pore

Throat and Mobilization Upon Contact with a Surfactant," (1983), **23,** 99-114.

[17] Chatzis, I. and Dullien, F. A. L.: "Dynamic Immiscible Displacement Mechanisms in Pore Doublets: Theory Versus Experiment," (1983), *J. Colloid Int. Sci.,* **91,** 199-222.

[18] Chatzis, I., Morrow, N. R. and Lim, H. T.: "Magnitude and Detailed Structure of Residual Oil Saturation," Paper SPE/DOE-10681, presented at the 3rd Symposium on Enhanced Oil Recovery, Tulsa, April 4-7, 1982.

[19] Wardlaw, N. C.: "The Effects of Pore Structure on Displacement Efficiency in Reservoir Rocks and in Glass Micromodels," paper SPE-8843, presented at the 1st Symposium on Enhanced Oil Recovery, Tulsa, April 20-23, 1980.

[20] Wardlaw, N. C and McKellar, M.: "Mercury Porosimetry and the Interpretation of Pore Geometry in Sedimentary Rocks and Artificial Models," (1981), *Powder Tech.,* **29,** 127-143.

[21] McKellar, M. and Wardlaw, N. C.: "A Method of Making Two-Dimensional Glass Micromodels of Pore Systems," (1982), *J. Canad. Petr. Tech.,* **21.**

[22] Bonnet, J. and Lènormand, R.: "Realisation de micromodeles pour l'etude des ecoulements polyphasiques en milieu poreux," (1977), *Rev. Inst. Franc. Petr.* **42,** 447-480.

[23] Mahers, E. G. and Dawe, R. A.: "The Role of Diffusion and Mass Transfer Phenomena in the Mobilization of Oil During Miscible Displacement," 2nd European Symposium on Enhanced Oil Recovery, Paris, September 8-11, 1982, 279-288.

[24] Lenormand, R., Cherbuin, C. and Zarcone, C.: "Interpretation d'experiences de retrait de mercure dans un reseau de capillaires," (1983), *C. R. Acad. Sci.,* Paris, **297,** 637-640.

[25] Lenormand, R. and Zarcone, C.: "Description des mecanismes d'imbibition dans un reseau de capillaires," (1983), *C. R. Acad. Sci.,* Paris, **297,** 393-396.

[26] Lenormand, R., Zarcone, C. and Sarr, A.: "Mechanisms of the Displacement of One Fluid by Another in a Network of Capillary Ducts," (1983), *J. Fluid Mech.,* **135,** 337-353.

[27] Larson, R. G., Scriven, L. E. and Davis, H. T.: "Percolation Theory of Two-Phase Flow in Porous Media," (1980), *Chem. Eng. Sci.,* **36,** 57-73.

[28] Lenormand, R. and Zarcone, C.: "Growth of Clusters During Imbibition in a Network of Capillaries," to appear in Proceedings of the Intern. Conf. on Kinetics of Aggregation and Gelation, Athens, April 2-4, 1984, edited by Landau D. P. and Family F.

[29] Morrow, N. R. and Songkran, B.: "Effects of Viscous and Buoyancy Forces on Nonwetting Phase Trapping in Porous Media," *Surface Phenomena in Enhanced Oil Recovery,* edited by Dinesh O. Shah, Plenum Publishing Corporation, 1981.

[30] Mayer, F. J., McGrath, J. F. and Steele, J. W.: "A Class of Similarity Solutions for the Nonlinear Thermal Conduction Problem," (1983), *J. Phys.* A, **16,** 3393-3400.

APPENDIX 1
FLOW ALONG THE ROUGHNESS

We begin by modeling the irregular space of the roughness of the duct walls by a regular bundle of capillaries. The roughness size is characterized by the length r, equal to the capillary diameter and distance between two of them (Fig. 13).

We also assume that there is no flow along the corners of the duct (this kind of flow will be studied in a separate calculation in Appendix 2) and the pressure drop is negligible for both fluids for the flow in the bulk of the duct. The nonwetting phase pressure is taken as reference, so the pressure in the wetting phase is negative.

Two kinds of boundary condition at the entrance of the duct are studied: constant flow rate and constant pressure.

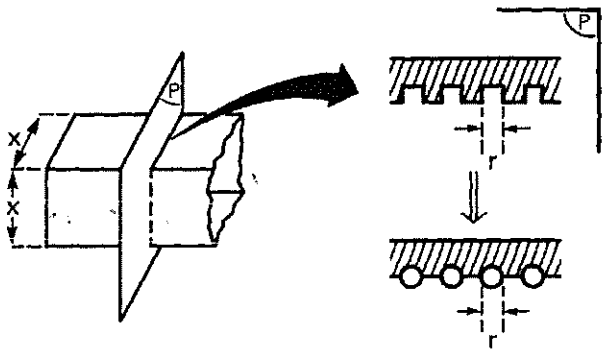

FIG. 13 - Modeling the roughness by circular cross-section capillaries.

Constant Pressure

The pressure P_0 of the wetting fluid at the entrance remains constant (for instance by using a capillary membrane and a constant negative level in the wetting fluid). This condition is stable only if a meniscus cannot be formed and move in the duct (see the conditions of stability of the interfaces), so the pressure must satisfy the relation:

$$P_0 < -\frac{4\gamma}{x} \tag{18}$$

The capillary pressure ($P_c = P_{nw} - P_w$) across the front meniscus in each small capillary is given by the Laplace law:

$$P_c = \frac{4\gamma}{r} \tag{19}$$

so, the pressure drop $\Delta P = P_0 - P_w$ in the capillary is given by:

$$\Delta P = 4\gamma\left(\frac{1}{r} - \frac{1}{x}\right) \tag{20}$$

And, assuming the size r of the roughness is smaller than x:

$$\Delta P = \frac{4\gamma}{r} \tag{21}$$

The volume flow rate q in each capillary is related to the pressure drop and the length l of the wetting fluid by the Poiseuille Law:

$$\Delta P = \frac{128\,\mu}{\pi\, r^4}\, q\, l \tag{22}$$

The wetting fluid is incompressible, so:

$$q = \frac{\pi\, r^2}{4}\,\frac{dl}{dt} \tag{23}$$

The classical result (Washburn equation) is deduced from these three equations:

$$l = \frac{1}{2}\left(\frac{\gamma\, r}{\mu}\right)^{\frac{1}{2}}\, t^{\frac{1}{2}} \tag{24}$$

and the flow rate in each capillary by:

$$q = \frac{\pi}{16}\left(\frac{\gamma}{\mu}\right)^{\frac{1}{2}}\, r^{\frac{5}{2}}\, t^{-\frac{1}{2}} \tag{25}$$

The total flow rate in the duct ($2x/r$ capillaries) is:

$$q_r = \frac{\pi}{8}\left(\frac{\gamma}{\mu}\right)^{\frac{1}{2}}\, x^{\frac{5}{2}}\left(\frac{r}{x}\right)^{\frac{3}{2}}\, t^{-\frac{1}{2}} \tag{26}$$

Constant Flow Rate

The volume flow rate q_0 of the wetting fluid injected in the duct is constant (with a pump for instance). A meniscus appears at the entrance of the duct and begins to move at time t_0.

- $t < t_0$. At the beginning of the displacement all the injected fluid flows along the roughness with a constant flow rate q (dotted zone, Fig. 14a).

$$q = q_0\,\frac{r}{2x} \tag{27}$$

The pressure P (negative) in the wetting phase increases as:

$$P + \frac{4\gamma}{r} = \frac{128\,\mu}{\pi\, r^4}\, q\, l \tag{28}$$

The fluid starts to flow in the bulk of the duct when the threshold pressure $P = 4r/x$ is reached at time t_0 (Fig. 14b). Using the assumption $r \ll x$, the capillary number notation (in the duct) and the following dimensionless variables:

$$y^* = 8\,Ca\,\frac{l}{r} \tag{29}$$

$$t^* = 8\,Ca\,\frac{q_0}{r\,x^2}\,t \tag{30}$$

the threshold is:

$$l_0^* = \frac{\pi}{2}\,\frac{r}{x} \tag{31}$$

$$t_0^* = \left(\frac{\pi}{2}\right)^2 \left(\frac{r}{x}\right)^2 \tag{32}$$

- $t \geq t_0$. The wetting fluid flows in the duct (hatched zone, Fig. 14c) with the flow rate q_d

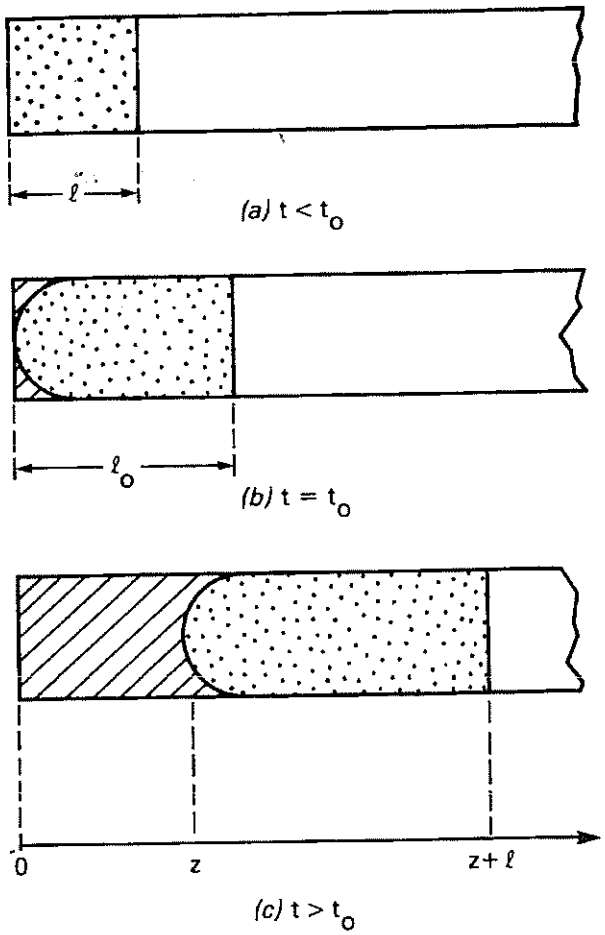

FIG. 14 - Flow in a single channel: along the roughness (dotted zone) and the bulk of the duct (hatched zone).

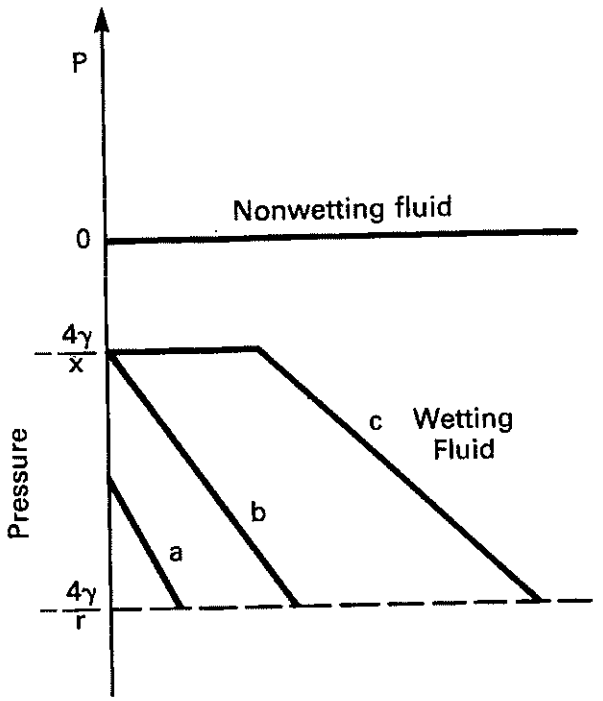

FIG. 15 - Pressure diagram in the channel (constant flow rate).

$$q_0 = q_d + 2\,\frac{x}{r}\,q \tag{33}$$

and, also, by definition of the flow rate:

$$q_d = S\,\frac{dz}{dt} \tag{34}$$

$$q = s\,\frac{d(z+l)}{dt} \tag{35}$$

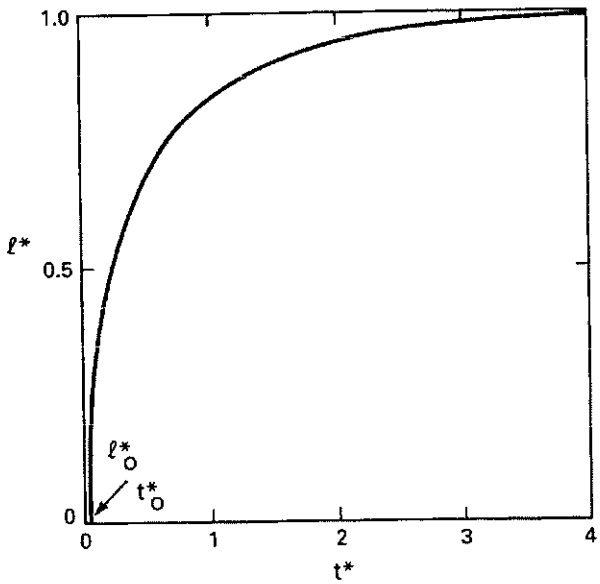

FIG. 16 - Dependence of roughness flow length on time (dimensionless variables).

In these equations s and S are the cross-section area of the small capillary and the duct. We introduce η, the ratio between the total area of the capillaries and the duct area ($\eta = n\ s/S$). The diagram, Fig. 15, shows the pressure in the wetting phase for the three cases (a,b,c) shown in Fig. 14.

The capillary pressure is equal to the pressure drop in the capillaries (only with a distance l; there is no pressure drop in the part of roughness where the duct is filled)

$$\frac{128\ \mu}{\pi\ r^4}\ q\ l = 4\ \frac{\gamma}{r} \tag{36}$$

The previous relations lead to the differential equation:

$$l^* + l^*\ \frac{dl^*}{dt^*} = 1 + \eta \tag{37}$$

After integration with the initial condition t_0^*, l_0^* and with the assumption $\eta \ll 1$:

$$t^* - t_0^* = l_0^* - l^* - \mathrm{Log}\ \frac{1-l^*}{1-l_0^*} \tag{38}$$

This function is plotted in Fig. 16. For $t^* > 3$, l^* reaches the asymptotic limit 1, in this case the length l of the flow along the roughness remain constant. Also, for these large value of time, the initial value t_0 and l_0 are close to zero. So, the asymptotic length l_∞ is given by:

$$l_\infty = \frac{1}{8\ Ca}\ r \tag{39}$$

APPENDIX 2
FLOW ALONG A CORNER

We consider only one corner (or dihedral) formed by the intersection of two planes. The origin is O and the length is infinite in the x direction (Fig. 17).

The wetting fluid is injected at the origin and we assume that we can control the boundary condition (constant flow rate or constant pressure).

Let us write the equations of the wetting fluid flow in the corner. We assume that the pressure drop in the nonwetting phase is negligible.

With the assumption of a very large radius of curvature in the plane parallel to the axis Ox and a zero contact angle, the shape of the meniscus in the cross-section, (Fig. 17), is a fraction of circle with a radius y linked to the pressure P and the surface tension γ by the Laplace law:

$$P(x) = -\frac{\gamma}{y(x)} \tag{40}$$

The wetting fluid is noncompressible, consequently the flow rate variation between x and $x + dx$ is equal to the volume variation:

$$\frac{\partial q}{\partial x} = -\frac{\partial S}{\partial t} \tag{41}$$

where q is the volume flow rate and S the area of the wetting fluid cross-section. By calculating S as a function of y :

$$\frac{\partial q}{\partial x} = -2\left(1 - \frac{\pi}{4}\right) y\ \frac{\partial y}{\partial t} \tag{42}$$

The pressure drop is calculated by using the approximations of the Poiseuille law and Hydraulic Diameter D_h and we neglect viscous forces at the interface between wetting and nonwetting fluid (influence of this term is studied in Reference 15).

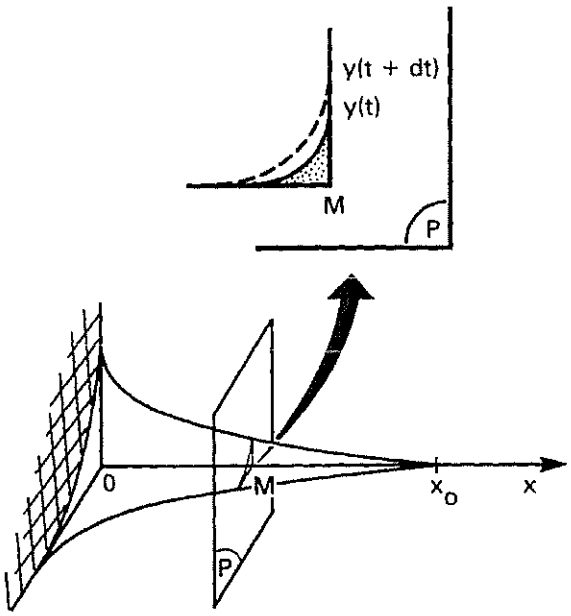

FIG. 17 - Flow along a corner. Shape of the meniscus.

$$D_h = 2\ y\left(1 - \frac{\pi}{4}\right) \tag{43}$$

$$\frac{\partial P}{\partial x} = \frac{128\, q\, \mu}{\pi\, D_h^4} \tag{44}$$

by eliminating P and q between these equations:

$$y\,\frac{\partial y}{\partial t} = D\,\partial\left[y^2\frac{\partial y}{\partial x}\right] \tag{45}$$

with:

$$D = \frac{\pi}{256}\left(1-\frac{\pi}{4}\right)^3\frac{\gamma}{\mu} \tag{46}$$

The numerical term in the coefficient D is linked to the angle between the two planes of the corner. Its value is about 3.9×10^{-5}.

An approximate solution of this nonlinear diffusion equation has been found by analogy with a nonlinear thermal problem. The calculation for different boundary conditions equivalent to constant pressure, constant flow rate and instantaneous deposition of fluid are detailed in Reference 30. We will give a summary of the case with a constant pressure P_0 at the origin (equivalent to a constant radius of curvature y_0). We seek self-similar solutions with the form:

$$y(x,t) = y_0[\,1-au\,+(a-1)u^2] \tag{47}$$

with the adimensional variable u defined by:

$$u = \frac{x}{b\,(1+2\nu t)^{\frac{1}{2}}} \tag{48}$$

The front of the wetting fluid, located at $x = x_0$, correspond to the value $u = 1$ and the condition of zero contact angle leads to $a = 2$.

The parameter b is calculated by a variational method (by minimizing the difference between the exact and approximate solutions) and ν is given by the initial shape of the meniscus. We assume that at $t = 0$ the lengh x_0 is equal to the dimension y_0. So, the solution is:

$$y = y_0\left[1-\frac{x}{y_0(1+2\nu t)^{\frac{1}{2}}}\right]^2 \tag{49}$$

with

$$\nu = \frac{15}{2}\frac{D}{y_0} \tag{50}$$

The flow rate q_0 at the entrance is given by:

$$q = 5.4 \times 10^{-4}\,\frac{\gamma}{\mu}\,\frac{y_0^2}{(1+2\nu t)^{\frac{1}{2}}} \tag{51}$$

For the large values of time ($\nu t \gg 1$) the previous equation become:

$$q = 2.2 \times 10^{-2}\left(\frac{\gamma}{\mu}\right)^{\frac{1}{2}} y_0^{\frac{5}{2}}\, t^{-\frac{1}{2}} \tag{52}$$